bioRxiv preprint doi: https://doi.org/10.1101/523365; this version posted January 17, 2019. The copyright holder for this preprint (which was not certified by peer review) is the author/funder, who has granted bioRxiv a license to display the preprint in perpetuity. It is made available under aCC-BY 4.0 International license.

Gene Expression Predictions and Networks in Natural Populations Supports the Omnigenic Theory

Aurélien Chateigner[1*]; Marie-Claude Lesage-Descauses[1]; Odile Rogier[1]; Véronique Jorge[1]; Jean-Charles Leplé[2]; Véronique Brunaud[3,4] ; Christine Paysant-Le Roux[3,4] ; Ludivine Soubigou-Taconnat[3,4] ; Marie-Laure Martin-Magniette[3,4,5] ; Leopoldo Sanchez[1*]; Vincent Segura[1*]

[1] *BioForA, INRA, ONF, Orléans, France*

[2] *BIOGECO, INRA, Univ. Bordeaux, Cestas, France*

[3] *Institute of Plant Sciences Paris-Saclay (IPS2), CNRS, INRA, Université Paris-Sud, Université d'Evry, Université Paris-Saclay, Bâtiment 630, Plateau de Moulon, Gif sur Yvette, France*

[4] *Institute of Plant Sciences Paris-Saclay (IPS2), CNRS, INRA Université Paris-Diderot, Sorbonne Paris-Cité, Bâtiment 630, Plateau de Moulon, Gif sur Yvette, France*

[5] *MIA-Paris, AgroParisTech, INRA, Paris, France*

* Equal contribution

Abstract

The recently proposed omnigenic model makes use of network theory to distinguish central (or core) from peripheral genes underlying phenotypes. Core genes are typically few, they marginally contribute highly but altogether explain only a small part of trait heritability, while peripheral genes, each of small influence, are so numerous that they finally lead risk. In order to test this model, we collected and sequenced RNA from 459 European black poplars. We built the coexpression networks to define core and peripheral genes as the most and least connected ones. We computed the role of each of these gene sets in the prediction of phenotypes, with a linear additive model and an interactive neural network model. These analyses showed that core genes act directly and contribute additively to phenotypes, consistent with a downstream position in a biological cascade. Oppositely, peripheral genes interact to influence phenotypes, consistent with an upstream position. Overall, our work is the first empirical proof that omnigenic holds in trees, providing one step further towards the universalization of this model.

bioRxiv preprint doi: https://doi.org/10.1101/523365; this version posted January 17, 2019. The copyright holder for this preprint (which was not certified by peer review) is the author/funder, who has granted bioRxiv a license to display the preprint in perpetuity. It is made available under aCC-BY 4.0 International license.

Introduction

In a recent study, Boyle, Li, and Pritchard[1] proposed the omnigenic theory, as an extension of the classic polygenic view for the genetic architecture of complex traits. They provide a clear but human-centered definition of their new paradigm explaining that numerous genes that are peripheral in a regulatory network are sufficiently connected to genes directly involved in a disease to modulate their effect and recover most of the missing heritability of the disease risk[2]. They conclude by inviting the community to test this hypothesis with empirical data. For that matter, the most obvious approach would be to infer gene networks and study the role of modules of different topologies in the definition of phenotypes. In the present study, we are not only going to test this theory with real empirical data, demonstrating the importance of centrality in the prediction of phenotypes but also extending the range of application to another kingdom: plants.

Two studies published just before Boyle's were already framing the subject within the plant kingdom. Josephs *et al*.[3] studied the link between previously published concepts related to gene expression[4], gene connectivity[5], divergence[6] and traces of natural selection[4,7]. They showed that both connectivity and proximity on the genome are important factors, while not being able to disentangle which of them is directly responsible for patterns of selection between genes. A week after, Mahler *et al*.[8] recalled the importance of studying the general features of biological networks in natural populations. With a genome-wide association study (GWAS) study on expression data from RNA sequencing (RNAseq), they suggested that purifying selection is the main mechanism maintaining the connectivity of core genes in a network and that this connectivity is inversely related to eQTLs effect size. These studies start to outline the first elements of the omnigenic theory, stating that core genes, which are highly connected, are each of high importance, and thus highly constrained by selection. On the opposite side of the network, there are peripheral, less connected genes, never far from a core hub, and each of low importance. These peripheral genes are less constrained genes and consequently, they harbor larger amounts of variation at population levels, concording with the omnigenic theory.

Classic studies of molecular evolution in biological pathways showed that selection pressure is correlated to the gene position within the pathway, either positively[9–14] or negatively[14–17], depending on the pathway. Jovelin & Phillips[17] showed that selective constraints are positively correlated to expression level, confirming previous studies[18–20]. Montanucci *el al.*[21] showed a positive correlation between selective constraints and connectivity, although such possibility remained contentious in previous works[22,23]. While Josephs' and Mahler's studies framed the general view behind Boyle's theory, based on topological features described in studies on molecular evolution of biological pathway, the respective roles of core and peripheral genes in the definition of a phenotype remain unclear. A more direct demonstration of those respective roles would be to predict phenotypes with different datasets representing the differences in the topology of the gene network. Even if predictions are still one step before in vivo experiments, they already represent a landmark that is not only correlative but also closer to causation, depending on the modeling strategy.

Our present study aims at exploring gene ability to predict traits, with datasets representing core genes and peripheral genes. We are using two methods to predict these phenotypes, a classic

bioRxiv preprint doi: https://doi.org/10.1101/523365; this version posted January 17, 2019. The copyright holder for this preprint (which was not certified by peer review) is the author/funder, who has granted bioRxiv a license to display the preprint in perpetuity. It is made available under aCC-BY 4.0 International license.

additive linear model, and a more complex and interactive neural network model in order to reflect the mode of action of each type of genes. On one hand, genes that are better predictors with an additive model are supposed to have an additive, direct mode of action representing a gene that would be downstream in a biological pathway. We expect core genes to display such additive behavior, with a high but selectively constrained expression level[17,21]. On the other hand, genes being better predictors with an interactive model are expected to be upstream in pathways. We expect peripheral genes to behave interactively, with a lower but relatively more variable expression level. With a lower variation, we also expect the core genes to be worse predictors for traits than peripheral genes unless larger effects can compensate it but a question remains whether it is a matter of trait category or whether the variation is anyway low.

To answer to these questions and thus empirically test the omnigenic theory, we have sequenced the RNA of 459 samples of black poplar (*Populus nigra*), corresponding to 241 genotypes, from 11 populations representing the natural distribution of the species across Western Europe. We also have for each of these trees phenotypic records for 17 traits, covering growth, phenology, physical and chemical properties of wood. They cover two different environments where the trees were grown in common gardens, in central France and northern Italy. By predicting these traits from our gene expression data, from different gene sets, selected based on their topology in networks, we are going to uncover the importance of genes of varying centrality in order to test the omnigenic theory.

Results

Wood samples, phenotypes, and transcriptomes

Wood collection and phenotypic data (**Table S1**) have been previously described[24]. Further details are provided in the methods section. Briefly, we are focusing on 241 genotypes planted in 2 common gardens, in Orléans (central France) and Savigliano (northern Italy), and for which phenotypic data have been collected. In Orléans, we used 2 clonal trees per genotype to sample xylem and cambium during the 2015 growing season for RNA sequencing. We mapped the sequencing reads on the *Populus trichocarpa* transcriptome (v3.0) to obtain gene expression data.

Data collection extended on a 2 weeks period, with varying weather along the days, and different operators involved. We did PCA analyses on the cofactors that were presumably involved in the experience, to look whether any confounding effect could be identified (**Figure S1**). No clear segregation was found for any of these, except for the ones associated with weather. To verify this observation, we used mixed-models to correct effects of all these cofactors, with the breedR R package[25], and while it properly corrected the environmental effects, it also removed information from the data, making prediction quality much poorer than without cofactor correction for most of the traits (**Figure S2**). Since phenotype is a mixture between genotype and environment, we supposed that correcting the environment also removed natural variation. Further analyses with complex neural network models, expected to account more efficiently for interactions with hidden theoretical states, did not show better results than additive models. We thus did not favor one particular type of model with

bioRxiv preprint doi: https://doi.org/10.1101/523365; this version posted January 17, 2019. The copyright holder for this preprint (which was not certified by peer review) is the author/funder, who has granted bioRxiv a license to display the preprint in perpetuity. It is made available under aCC-BY 4.0 International license.

uncorrected data. Moreover, we did not aim at interpreting the effect of each variable in this study but rather at inferring mechanisms from the prediction quality of the different models, which might be less prone to confounding effects.

From the 41,335 transcripts obtained from the mapping, we removed the 1,653 without reads, we normalized the read counts, stabilized their variance and transformed the counts of the 39,682 remaining transcripts to counts per million. Further details are provided in the methods section. Hereafter, we refer to this set of 39,682 transcripts as the full gene set (96% of annotated transcripts).

Clustering and network construction

The classical approach to build a signed scale-free gene expression network is to use the weighted correlation network analysis (implemented in WGCNA R package[5]), using a power function on correlations between gene expressions. We chose to use Spearman's rank correlation to avoid any assumption on the linearity of relationships. The scale-free topology fitting index (R^2) reached a maximum of 0.85 for a soft threshold of 15, yielding a mean connectivity of 22.9 (**Figure 1A**). We detected 25 gene expression modules (**Table S2**) with automatic detection (merging threshold: 0.25, minimum module size: 30, **Figure 1B**). Spearman correlations between 17 traits values and expression, presented in the lower panel of the **Figure 1B** below the module membership of each gene, display a structuration when ordered following the gene expression tree. The traits themselves are line ordered according to clustering on their scaled values to represent their relationships (**Figure S3**). Interestingly, some patterns in the correlation between expression and traits do not follow what we would expect from the similarity between traits (3 traits out of 7 with data in both sites). For instance, in the group composed of S/G ratios and glucose composition, the patterns were more similar between sites across traits than between traits across sites (**Figure 1B and S3**). Complex shared regulations mediated by the environment seem to be in control of these phenotypes, suggesting site-specific genetic control. Otherwise, glucose composition in Savigliano, infra-density, and extractives in Orléans presented similar patterns, contrarily to what would be expected from the correlations between these traits. These results suggest that the comparative analysis of correlations between gene expression and between traits allow unraveling underlying links between traits that are not obvious from factual phenotypic and genetic correlations between traits.

To get further insight into the relationships between module composition and traits, we looked at the strongest correlations between the best theoretical representative of a gene expression module (eigengene) and each trait, in order to identify genes in relevant modules with an influence on the trait (**Figure 1C**). Following a Bonferroni correction of the p-values provided by WGCNA, only 72 correlations remained significant ($p \leq 0.05$) out of the initial 425 traits by modules combinations, and 5 modules were defined as composed of genes not involved in any of the traits studied (salmon, greenyellow, brown, lightgreen and darkgrey, **Figure S4**). In significantly correlated modules, gene expression correlation with trait was also significantly correlated with centrality in the module (represented by the kME, the correlation with the module eigengene), while no correlation was found in poorly correlated modules (**Figure 1D**, **Figure S5**). In other words, there is a three-way correlation. The genes with the highest kME in a given module are the most correlated to the eigengene and, consequently, are also the most

bioRxiv preprint doi: https://doi.org/10.1101/523365; this version posted January 17, 2019. The copyright holder for this preprint (which was not certified by peer review) is the author/funder, who has granted bioRxiv a license to display the preprint in perpetuity. It is made available under aCC-BY 4.0 International license.

correlated to those traits with the largest correlation with the module eigengene. Although this is somehow expected, it underlines the usefulness of kME as a centrality score to further characterize the genes within each module. We thus used this centrality score to define further the topological position of our gene expressions in networks. In order to avoid bias in gene selection by large groups, we selected the 10% of genes with the highest global absolute scores to define the "core genes" group, and the 10% with the lowest global absolute scores to define the "peripheral genes" group. Finally, we selected 100 samples of 3968 "random genes" as control groups (**Figure S6**).

One particular module in the resulting clustering is the grey module. This module typically gathers genes with poor membership to any other module. In our case, it is the largest module, with 15214 genes (38% of the full set), it gathers the vast majority of genes with very low kME (**Figure S6**) and 99% of the peripheral genes set (**Table S4**). While it is typically discarded in classic clustering studies, its eigengene displays the highest number of significant correlations with traits suggesting non-negligible biological roles (**Figure 1C, Figure S4**). It thus appears interesting to use it as a contrasting set for the remaining of the study in the light of the omnigenic theory.

To assess the robustness of WGCNA analysis results, we compared it to a k-means clustering (R package coseq[25]) of the gene expressions (**Figure S7A**). The distribution of WGCNA and k-means' clusters showed a correlation of 0.42 (**Figure S7B**). K-means clustering forces groups of comparable size, which does not seem biologically credible. Furthermore, the correlations between the k-mean modules eigengenes and traits were lower than with WGCNA's, with a poor repartition of the different modules on the first 2 principal component analysis space (**Figure S7C**). We thus preferred WGCNA clustering to k-means clustering for this analysis and were quite confident about its robustness given its overall concordance with k-means clustering.

Boruta gene expression selection

In addition to previous gene sets building (full, core, random, peripheral), we wanted to have a set of genes being relevant for their predictability of the phenotype. Our hypothesis here would be that this set is the one that enables the best prediction of a given trait with a limited gene number that would be comparable to the other subsets of genes selected on their characteristics within the networks. For that purpose, we performed a Boruta (Boruta R package[26]) analysis on the full genes set. This algorithm performs several random forests to analyze which gene expression profile is important to predict a phenotype. In the end, a pool of 637 unique gene expressions was found to be important to predict our phenotypes (**Figure S8**). Traits with the highest number of important genes are related to growth. For the other traits, we always have more genes selected when the trait is measured in Orléans compared to Savigliano (respective medians of 29 and 17.5). We hypothesize that this is due to the fact that RNA extraction was performed on trees in Orléans. One exception to this pattern is the Lignin content, that we suspect to be due to a methodological difference between assessments, as previously discussed[24]. On average, genes that were specific to single traits represented 62% of selected genes, genes shared across sites for a given trait were 4%, genes shared by trait category (growth, phenology, physical, chemical) were 18%, and genes shared among all traits were 16%.

bioRxiv preprint doi: https://doi.org/10.1101/523365; this version posted January 17, 2019. The copyright holder for this preprint (which was not certified by peer review) is the author/funder, who has granted bioRxiv a license to display the preprint in perpetuity. It is made available under aCC-BY 4.0 International license.

Phenotype prediction with gene expression

For our 5 genes sets (full, core, random, peripheral and Boruta), we trained two classes of models to predict the phenotypes: an additive linear model (ridge regression) and an interactive neural networks model. For the former, we used ridge regression to avoid overfitting problems. For the latter, we chose neural networks as a contemporary machine-learning method, which is not subjected to dimensionality problems[27] and is able to capture interactions without *a priori* explicitation between the entries, here gene expressions. **Figure 2** and **S9** show that for linear modeling with ridge regression, the best genes set to predict phenotypes was the core gene set, followed by the full, Boruta, random and peripheral sets (respective median prediction R^2 over all traits of 0.33, 0.31, 0.25, 0.18 and 0.16). On the contrary, for neural network modeling, core genes constituted the worst set by far, followed by a cluster of similarly performing peripheral, random and Boruta sets (respective median prediction R^2 over all traits of 0.07, 0.21, 0.22, 0.22). We have not been able to compute neural network models with the full set as the number of predictors remains too large to be fitted within a reasonable time on computing clusters. Across phenotypes (**Figure S9**), predictions were generally less variable under neural network than under the ridge regression counterpart (interquartile range mean division by 1.48).

To further investigate the behavior of genes with different positions in networks with respect to the prediction model used, we computed differences between prediction scores for core and peripheral gene sets for additive (ridge regression) and interactive (neural network) algorithms (**Figure 3**). As a null reference for inference, a randomization strategy involving 100 random sets of genes was used to infer differences in prediction scores between models due to random sampling. For this, we computed a total of 4950 differences corresponding to all pairwise differences, excluding reciprocals and self-comparisons. A positive difference indicates an advantage of core genes sets over peripherals and, conversely, a negative difference indicates an advantage of peripheral genes. Except for 4 out of 17 cases, most traits showed a contrasting behavior of the two alternative algorithms. While most additive ridge regression models yielded positive scores across traits, the neural network counterpart showed negative scores. This hints at the fact of different gene actions in the two sets of genes. Indeed, the former ridge regression models capture mostly additive gene actions, which appeared to be prominent for core genes. Contrarily, neural network modeling is better suited for revealing gene interactions, which seem to be inherently associated with peripheral gene functioning. On average, the neural network has a mean difference of -0.08, showing that they are mainly in favor of the peripheral genes set. On the opposite, ridge regression models have mean differences of 0.24, showing that they are predicting a lot better with core genes set. It should be noted that concording behavior may come from the almost complete inability to predict the phenotype for a particular trait (a score close to 0 in **Figure 2**). In most of the cases, the contrasty pattern between core and peripherals with the two algorithms could not be drawn exclusively by chance as indicated by the distribution of randomized sets which clearly appears to be centered on zero (mean differences of -0.002 and 0.0002 for neural network and ridge regression models respectively).

bioRxiv preprint doi: https://doi.org/10.1101/523365; this version posted January 17, 2019. The copyright holder for this preprint (which was not certified by peer review) is the author/funder, who has granted bioRxiv a license to display the preprint in perpetuity. It is made available under aCC-BY 4.0 International license.

Heritability and population differentiation of modules

To understand the biological role of core and peripheral genes at population levels, we computed gene expression level (Figure 4B), several classical population statistics (**Figure 4A, 4C, 4E, and 4F**) and a contemporaneous equivalent to F_{ST} for genome scans (**Figure 4D**). Gene expression level, heritability, Qst and coefficient of genetic variation were computed from gene expression data, while gene diversity and PCadapt scores[28] were computed from polymorphism data (SNP), for more details see the method section.

The extent of heritability for gene expression was higher for random the set than for core and peripheral genes, the latter having extremely low median heritability (0.04) (**Figure 4A**). Gene expression level (**Figure 4B**) and the extent of population differentiation from expression data (**Figure 4C**) tended to be higher in core set than in the other sets, with intermediate levels in the random set and the lowest levels in the peripheral set. According to PCadapt score (**Figure 4D**), core genes showed more evidence of population-specific selection patterns than the other two sets, with random genes having intermediate levels. Concerning the coefficient of genetic variation (**Figure 4E**), there was a clear difference between sets, with core genes displaying a very low variation, peripheral genes a very high, and random genes intermediate levels. Finally, there was a small difference in overall gene diversity (**Figure 4F**) that confirms the differences observed for CV_G computed on gene expression level, peripheral genes being more diverse than random, and random more diverse than core genes.

Altogether, these statistics showed clear differences between core and peripheral genes: core genes are highly expressed (**Figure 4B**), highly differentiated between populations (**Figure 4C**), with generally low levels of genetic variation (**Figure 4D, 4E, 4F**); while peripheral genes are poorly expressed, poorly differentiated between populations, with generally higher genetic variations.

Discussion

Omnigenic theory[1] states that in gene regulatory networks, highly connected core genes are of high importance individually but altogether explain only a small part of heritable phenotypic variation, while peripheral genes, each of low importance and connectivity, altogether explain the majority of phenotypic variation. This theory, enunciated with human diseases in mind, needed to be tested with empirical data and broadened to other kingdoms of life.

In order to contribute to the empirical support of the omnigenic theory, we studied in *Populus nigra* the role and predictive ability of 2 gene sets, on opposite sides of a gene coexpression network. We defined core and peripheral genes as the 10% most central and most peripheral genes respectively according to the outputs of WGCNA analysis. We are aware that this is somehow an oversimplification, an extreme contrast of an otherwise continuous phenomenon. Moreover, according to the omnigenic theory, core genes are only a “modest number” and peripheral genes are the remaining majority of expressed genes. While the choice of the arbitrary threshold of 10% is based on the Mahler’s definition of core genes[8], the fact of equaling both samples responded to the need for statistical comparativeness between equivalent samples. Moreover, such contrasting samples represented two conspicuous features of the distribution of kME (**Figure S6**), with a thick tail of well-connected genes and a high mass

bioRxiv preprint doi: https://doi.org/10.1101/523365; this version posted January 17, 2019. The copyright holder for this preprint (which was not certified by peer review) is the author/funder, who has granted bioRxiv a license to display the preprint in perpetuity. It is made available under aCC-BY 4.0 International license.

of poorly connected genes. The outputs of WGCNA analysis on which our gene discrimination is based provided better results than k-means clustering. It has to be noted that k-means forces clusters to be of equal size, which could restrain concordance and ultimately does not reflect biological reality. In addition, we selected these modules on normalized gene counts for which we only stabilized the variance. No further correction of data could be done without reducing the prediction signal, thus we have to consider that environmental conditions while showing a low impact, are not corrected for the present analysis. Despite this environmentally uncorrected data, clusterings with two methods remain concordant, somehow pinpointing the robustness of the outcome in gene classification.

On average, core genes were the ones predicting the most efficiently a phenotype, for any trait category, with an additive model, even if the full set still reaches the highest global prediction R^2 (0.77 for the mean sample diameter). This might be expected from the positive and highly significant relationship observed between gene significance and connectivity within WGCNA modules displaying a significant correlation with traits. On the other side of networks, peripheral genes predict better with an interactive model than with an additive one and provide over both types of models the most stable predictions (interquartile ranges of 0.19 for peripheral, 0.27 for random, 0.34 for core and Boruta and 0.35 for full set). The information necessary to predict a phenotype does not seem to be particularly concentrated at any side of the network, but rather spread over it, as highlighted by the performance of random gene sets. They capitalize enough information to perform predictions more accurately than an equal number of peripheral genes. Moreover, prediction with larger peripheral sets (20% and 30% of genes) confirmed that peripheral genes need to be in a high number to reach high prediction R^2, as the median doubled between 10% and 30% sets, but not necessarily with more central genes in the network as it tended to drop with 40% of genes (**Figure S10**, median R^2 of 0.15, 0.23, 0.33 and 0.29 respectively for 10%, 20%, 30% and 40% peripheral gene sets). In that sense, Boruta seems to be extremely useful to focus on the information that is relevant for prediction. From the 637 genes selected by Boruta, 95 and 22 were core and peripheral genes, respectively. If the number of core genes within the Boruta set is greater than expected by chance (Fisher's exact test p-value < 0.0001), a large majority of Boruta genes still do not belong to this category nor to the peripheral gene set. Boruta selection proved to be able to select a small number of genes for all of our phenotypes, allowing for a faster and more precise prediction, with less than one-sixth of genes compared to the core or peripheral sets, and only 1.6% of the full set, with predictions being almost as accurate. This makes Boruta an advantageous alternative in genomic evaluation for breeding to more classic methods (based on the imposition of a priori constraints for shrinkage or variable selection[29]) like ridge regression.

Tracking back predictabilities down to particular gene sets is an essential step before being able to understand the roles of interactivity and connectivity in a gene network underlying the phenotype. In that sense, the high levels of connectivity shown by core genes do not appear to be a prerequisite for prediction quality, while these particular genes find better fits in additive models. Contrarily, peripheral genes, while being poorly connected, display prediction quality equivalent to random or Boruta sets in interactive models. This pinpoints to an a priori paradoxical situation in which connectivity and interaction are not necessarily found in the same gene sets. Here, connectivity refers to the degree of membership of a given gene within a coexpression network and one should note that this was defined independently from the

bioRxiv preprint doi: https://doi.org/10.1101/523365; this version posted January 17, 2019. The copyright holder for this preprint (which was not certified by peer review) is the author/funder, who has granted bioRxiv a license to display the preprint in perpetuity. It is made available under aCC-BY 4.0 International license.

phenotype. Interactivity, on the other hand, refers to the way the expression profile of a given gene is mediated before affecting the phenotype. Such interactivity between gene expressions is quite different from what is usually referred to as epistasis in the genetics literature, the interaction effect between alleles from different loci on a given phenotype[30], because here the input is gene expressions instead of allelic polymorphisms. Weather connectivity or interactivity relates to epistasis is beyond the scope of current work, but clearly deserves further investigation. In order to clarify this apparent paradox, one hypothetical scenario could be proposed, following the model schematized in **Figure 5**. Basically, in this model, a peripheral gene is located upstream within biological pathways and it produces an essential brick which can be further modified or complemented by the bricks of subsequent genes downstream. The peripheral genes that produce essential bricks do it with a low connection to other genes. As we progress downstream within the pathways, the bricks from peripheral genes suffer a chain of subsequent modifications due to or controlled by other genes, resulting in an impact on the final phenotype that can be highly mediated by many intermediaries, appearing as interactors, that somehow blur the brick's contribution to the ultimate phenotype. This could explain the interactive behavior of peripheral genes, as sitting far away from the final phenotype, while being poorly connected. Core genes, on our schematic model, receive upstream bricks from many peripheral genes, and their output directly impacts or influence the phenotype. This may be a reason why core genes while being highly connected, behave additively, as they almost directly appear to contribute to the phenotype. We have further looked for enrichment in transcription factors (TFs) within the core and peripheral gene sets and found that TFs were overrepresented within the core gene set (Fisher's exact test p-value < 1.10^{-14}), while they were underrepresented within the peripheral gene set (Fisher's exact test p-value < 1.10^{-7}). This leads us to believe that core genes consist in fact of a mixture of highly connected regulators and genes downstream within biological pathways, which altogether contribute to the metabolic flow towards phenotypes. Consequently, they would behave additively when predicting a trait, they could contribute individually to a large proportion of phenotypic variation, and they could, therefore, suffer "first hand" the selection pressure. Core genes variation levels are low by comparison to their expression level and they might display distinct optima according to population structure, as underlined by their higher Qst and PCadapt scores in our data. As they depend much on other bricks, they have less room for variation, and are somehow "canalized". Peripheral genes, on the other hand, are highly variable with lower expression levels. They are thus the ones by which variations come to the network and propagate downstream. These observations are consistent with molecular evolution studies, as Jovelin *et al.*[17] showed a positive correlation between selective constraints and expression level and Fraser & Hirsh[23] showed that core genes are more expressed, but less variant compared to their expression. Finally, Montanucci *et al.*[21] showed a positive correlation between selective constraints and connectivity, which also echoes in our measures and models.

Our results have brought to the omnigenic theory new insights into the function and behavior of genes with respect to their position in the network, by an integrative approach combining predictive and explanatory functions. We also showed that the omnigenic theory holds within our Poplar dataset, leading us to think that this theory may be more ubiquitous than originally described. We believe that there is no apparent reason why it would not apply to the entire plant kingdom and everything that lays in-between humans and poplars on the tree of life. We are

bioRxiv preprint doi: https://doi.org/10.1101/523365; this version posted January 17, 2019. The copyright holder for this preprint (which was not certified by peer review) is the author/funder, who has granted bioRxiv a license to display the preprint in perpetuity. It is made available under aCC-BY 4.0 International license.

thus making a point here enlarging the omnigenic theory to not only humans as it was first described but to any living being complex enough to have gene networks.

Methods

Samples collection

As described in previous works[24,31], we established in 2008 a partially replicated experiment with 1160 cloned genotypes, in two contrasting sites in central France (Orléans, ORL) and northern Italy (Savigliano, SAV). At ORL, the total number of genotypes was of 1,098 while at SAV there were 815 genotypes. In both sites, the genotypes were replicated 6 times in a randomized complete block design. At SAV, the trees were pruned at the base after one year of growth (winter 2008-2009) to remove a potential cutting effect and were subsequently evaluated for their growth and wood properties during the winter 2010-2011. At ORL, the trees had the same pruning treatment after two years of growth (winter 2009-2010), and were also subsequently evaluated for growth and wood properties after two years (winter 2011-2012). After evaluation, they were pruned again for a new growth cycle. At their fourth year of growth (2015), 241 genotypes present in two blocks of the French site were selected to perform sampling for RNA sequencing. In the end, we obtained transcriptomic data from 459 samples. These 241 genotypes were representative of the natural west European range of *P. nigra* through 11 river catchments in 4 countries (**Table S3**).

We described 14 of the 17 phenotypic traits in a previous work[24]. Briefly, these traits can be divided into two categories, growth traits and biochemical traits which were all evaluated on up to 6 clonal replicates by genotype at each site after two years of growth. The first set is composed by the circumference of the tree at 1-meter height measured in Savigliano at the end of 2009 (CIRC2009.Sav) and in Orléans at the end of 2011 (CIRC2011.Orl). The second set is composed, each time at both sites, of measures of ratios between the different components of the lignin, p-hydroxyphenyl (H), guaiacyl (G) and syringyl (S) (H.G.Orl, H.G.Sav, S.G.Orl and S.G.Sav), measures of the total lignin content (Lignin.Orl : measure of the lignin in Orléans, Lignin.Sav: measure of the lignin in Savigliano), measure of the total glucose (Glucose.Orl and Glucose.Sav), measure of ratio between 5 and 6 carbon sugars (C5.C6.Orl and C5.C6.Sav) and measure of the extractives (Extractives.Orl and Extractives.Sav). For each of these traits, we computed mean values per genotype previously adjusted for microenvironmental effects (block or spatial position in the field).

The 3 remaining traits were measured in 2015 on the trees harvested for the RNA sequencing experiment (2 replicates per genotype). They include the mean diameter of the stem section harvested for RNA sequencing (MeanDiameter), the date of bud flush of the tree in 2015 (Date3Doy) and the basic density of the wood (Infraden). Date of bud flush consisted in a prediction of the day of the year at which the apical bud of the tree was in stage 3 according to the scale defined in Dillen *et al*.[32]. Predictions were done with a lowess regression from discrete scores recorded at consecutive dates in the spring of 2015. Wood basic density was measured on a piece of wood from the stem section harvested for RNA sequencing following the Technical

bioRxiv preprint doi: https://doi.org/10.1101/523365; this version posted January 17, 2019. The copyright holder for this preprint (which was not certified by peer review) is the author/funder, who has granted bioRxiv a license to display the preprint in perpetuity. It is made available under aCC-BY 4.0 International license.

Association of Pulp and Paper Industry (TAPPI) standard test method T 258 “Basic density and moisture content of pulpwood”.

Transcriptome data generation

We sampled stem sections of approximately 80 cm long starting at 20 cm above ground and up to 1 meter in June 2015. The bark was detached from the trunk in order to scratch young differentiating xylem and cambium tissues using a scalpel. The tissues were immediately immersed in liquid nitrogen and crudely ground before storage at -80°C pending milling and RNA extraction. Prior to RNA extraction, the samples were finely milled with a swing mill (Retsch, Germany) and tungsten beads under cryogenic conditions with liquid nitrogen during 25 seconds (frequency 25 cps/sec). About 100 mg of milled tissue was used to isolate separately total RNA from xylem and cambium of each tree with RNeasy Plant kit (Qiagen, France), according to manufacturer’s recommendations. Treatment with DNase I (Qiagen, France) to ensure elimination of genomic DNA was made during this purification step. RNA was eluted in RNAse-DNAse free water and quantified with a Nanodrop spectrophotometer. RNA from xylem and cambium of the same tree were pooled in an equimolar extract (250 ng/µl) before sending to the sequencing platform.
RNAseq experiment was carried out at the platform POPS (transcriptOmic Platform of Institute of Plant Sciences - Paris-Saclay) thanks to IG-CNS Illumina Hiseq2000. RNAseq libraries were constructed using TruSeq_Stranded_mRNA_SamplePrep_Guide_15031047_D protocol (Illumina®, California, U.S.A.). The RNAseq samples have been sequenced in single-end reads (SR) with an insert library size of 260 bp and a read length of 100 bases. Images from the instruments were processed using the manufacturer’s pipeline software to generate FASTQ sequence files. Ten samples by lane of Hiseq2000 using individually barcoded adapters gave approximately 20 millions of PE reads per sample. We mapped the reads on the *Populus trichocarpa* v3.0 transcriptome with bowtie2[33], and obtained the read counts for each of the 41,335 transcripts by homemade scripts. Initially, we considered using the genotype mean to reduce our data volume. However, differences between replicates were not normally distributed, because of variation in gene expression due to plasticity. We thus could not summarize our data with their mean, as it would have removed this information and finally we chose to keep replicates as separate data samples.

Filtering the non-expressed genes, normalization and variance stabilization

As the sampling ran along 2 weeks, we expected environmental variables to blur the signal. To understand how our data were impacted, we ran the first analysis, containing a step identifying the impact of each cofactor and a step correcting confounding effects, with mixed linear models implemented in the R package breedR[25]. However, while it was properly correcting the covariables that seemed to impact our data (environmental effects) when controlling on PCA spaces, it was also erasing useful information from the data, yielding less accurate prediction models than without any correction. We thus chose not to perform this correction, and use raw uncorrected data.

bioRxiv preprint doi: https://doi.org/10.1101/523365; this version posted January 17, 2019. The copyright holder for this preprint (which was not certified by peer review) is the author/funder, who has granted bioRxiv a license to display the preprint in perpetuity. It is made available under aCC-BY 4.0 International license.

We started cleaning our raw counts data by removing the transcripts with 0 counts for all individuals. From the original 41,335 genes, 1,653 were thus removed, leaving 39,682 genes with at least 1 count in at least 1 individual.
After this first filtration, we normalized the raw counts data by Trimmed Mean of M-values (TMM, edgeR[34]). As most features are not differentially expressed, this method takes into account the fact that the total number of reads can be strongly influenced by a low number of features. Then, we calculated the counts per millions (CPM[35]).
To stabilize the variance of the CPM data, we computed a log2(n+1) instead of a log2(n+0.5)[36] used in a voom analysis[35]. The reason is that the former avoids negative values, which are problematic for the rest of the analysis. The resulting data set is called "Full", these counts are also shown in **Figure 4B**.

Hierarchical and k-means clustering

We performed a weighted correlation network analysis with the R package WGCNA[5] on our full RNA sequencing gene set. We followed the classic approach, except that we first ranked our expression data, to work subsequently with Spearman's non-parametric correlations and avoid problems due to linear modeling assumptions. We first chose the soft threshold with the highest scale-free topology fitting index (R^2 = 0.85), which is for a power of 15 (connectivity: mean = 22.90, median = 8.94, max = 329, **Figure 1A**). Then, we used the automatic module detection (blockwiseModules function) via dynamic tree cutting with a merging threshold of 0.25, a minimum module size of 30 and bidweight midcorrelations (**Figure 1B**). All other options were left to default. This also computes module eigengenes. To order the traits, we clustered their scaled values with the pvclust R packages[37], the Ward agglomerative method ("Ward.D2") on correlations (**Figure 1B** and **C**, **Figure S3**). The clustering on euclidian distance results in the exact same hierarchical tree. Correlations between traits and gene expression or module eigengenes were computed as Spearman's rank correlations (**Figure 1B** lower panel and **1C**).
We also performed a k-means clustering with the R package coseq[38]: considering 10 initial runs, 1000 iterations, without any other data transformation, and for a number of clusters (K) between 2 and 20. At first, it identified a K without strong agreement between the two evaluation algorithms included in coseq. We computed additional rounds of k-means clustering, between K-5 and K+5, with 100 initial runs and 10000 iterations, until both evaluation algorithms agreed.

Machine learning

Boruta gene expression selection

In addition to the inconvenience of working with a large number of features (time and power consumption), most machine learning algorithms perform better when the number of predicting variables used is kept as low as the optimal set[39]. We thus performed an all relevant variable selection[40] with the Boruta function[26] from the eponym R package, with a 5% p-value threshold, on the full gene expression set, for each phenotype independently. Then, features that were not rejected by the algorithm were pooled together, so that all the important genes were in the selected gene pool.

bioRxiv preprint doi: https://doi.org/10.1101/523365; this version posted January 17, 2019. The copyright holder for this preprint (which was not certified by peer review) is the author/funder, who has granted bioRxiv a license to display the preprint in perpetuity. It is made available under aCC-BY 4.0 International license.

Models

Both additive linear model (ridge regression) and interactive neural networks models were computed by the R package h2o[41]. They both used the gene expression sets as predictors and one phenotypic trait at a time as a response. Gene sets were split by the function h2o.splitFrame in 3 sets, a training set, a validation set and a test set, with the respective proportions of 60%, 20%, 20%. Consequently, to evaluate model quality we used prediction accuracies reported as R^2 between observed and predicted values within the test set and using the function R2 of the R package compositions[42].

For linear models, we used the function h2o.glm with default parameters, except 2-folds cross-validation and alpha set at zero to perform a ridge regression.

Neural networks have the reputation to be able to predict any problem, based on the Universal approximation theorem[43,44]. However, this capacity comes at the cost of a very large number of neurons in one layer, or a reasonable number of neurons per layer in a high number of layers. Both settings lead to difficult interpretation when very many gene expressions are involved. In that sense, we chose to keep our models simple, with two layers of a reasonable number of neurons (see models architectures in Methods). This obviously comes at the price of lower prediction power. However, we believe that these topologies give us the power to model 2 levels of interactions between genes (1 level per layer). Furthermore, since both methods yielded comparable prediction R^2 (median ridge regression R^2 = 0.27, mean neural network R^2 = 0.22), this complexity seemed appropriate. To find the best models for neural networks, we computed a random grid for each response. We tested the following hyperparameters: (i) “Rectifier”, “Tanh”, “RectifierWithDropout” and “TanhWithDropout” activation. (ii) the network structure is based on the number of genes used as predictors (h). The first layer is composed of h, ⅔h or ⅓h neurons. The second layer has a number of nodes equal or lower to the first one and is also composed of h, ⅔h or ⅓h neurons. This represents 6 different structures. (iii) Input layer dropout ratio is 0 or 0.2. (iv) L1 and L2 regularization are comprised between 0 and $1x10^{-4}$, with steps of $5x10^{-6}$. We performed a random discrete strategy to find the best search criteria, computing a maximum of 100 models, with a stopping tolerance of $1x10^{-3}$ and 10 stopping rounds. Finally, h2o.grid parameters are the following: the algorithm is “deeplearning”, with 10 epochs, 2 fold cross-validation, maximum duty cycle fraction for scoring is 0.025 constraint for a squared sum of incoming weights per unit is 10. All other parameters have default values. The best model is selected from the lowest RMSE score within the validation set.

Heritability and Qst Models

A 12k bead chip[45] provided 7,896 SNPs in our population. A genomic relationship matrix between genotypes has been computed with these SNPs by LDAK[46], and further split into between (mean population kinship, K_b) and within population relationship matrices (kinship kept only for the members of the same population, all the others are equal to 0, K_w). These matrices, associated to design matrices, were used in a mixed linear model to compute an additive genetic variance between and within populations (equation 1) for the expression of each gene. In this model, y is a gene expression vector across individual trees, β_0 is a vector of fixed effects (overall mean or intercept); b and w are respectively random effects of populations and

bioRxiv preprint doi: https://doi.org/10.1101/523365; this version posted January 17, 2019. The copyright holder for this preprint (which was not certified by peer review) is the author/funder, who has granted bioRxiv a license to display the preprint in perpetuity. It is made available under aCC-BY 4.0 International license.

individuals within populations, which follow normal distributions, centered around 0, of variance $\sigma_b^2\mathbf{K_b}$ and $\sigma_w^2\mathbf{K_w}$, where σ_b^2 and σ_w^2 are the between and within population variance component and K_b and K_w are the between and within population kinship. Z_b and Z_w are known incidence matrices between and within populations, relating observations to random effects b and w. ϵ is the residual component of gene expression, following a normal distribution centered around 0, of variance $\sigma_\epsilon^2 I$, where σ_ϵ^2 is the residual variance and I is an identity matrix.

$$\mathbf{y} = \beta_0 + \mathbf{Z_b}\mathbf{b} + \mathbf{Z_w}\mathbf{w} + \epsilon \quad \text{(equation 1)}$$

From the between and within population variance components, we can compute heritability (h^2, equation 2) and population differentiation estimates (Q_{ST}, equation 3) for each gene. To compute them, we used the function remlf90 from the R package breedR[25], with the Expectation-Maximization method followed by one round with Average-Information algorithm to compute the standard deviations.

$\mathbf{b} \sim N(0, \sigma_b^2\mathbf{K_b})$; $\mathbf{w} \sim N(0, \sigma_w^2\mathbf{K_w})$; $\epsilon \sim N(0, \sigma_\epsilon^2\mathbf{I})$

$$h^2 = \frac{\sigma_b^2 + \sigma_w^2}{\sigma_b^2 + \sigma_w^2 + \sigma_\epsilon^2} \quad \text{(equation 2)}$$

$$Q_{st} = \frac{\sigma_b^2}{\sigma_b^2 + 2\sigma_w^2} \quad \text{(equation 3)}$$

We computed the genetic variation coefficient (CV_G) by dividing sums of σ_b^2 and σ_w^2 by expression mean, per gene.

Other population statistics

We further used a previously developed bioinformatics pipeline to call SNPs within our RNA sequences[47]. Briefly, this pipeline involves classical cleaning and quality control steps, mapping on the *Populus trichocarpa* v3.0 reference genome, and SNP calling using the combination of four different callers. We ended up with a set of 874,923 SNPs having less than 50% of missing values per genotype. The missing values were further imputed with the software FImpute[48]. We validated our genotyping by RNA sequencing approach by comparing the genotype calls with genotyping previously obtained with an SNP chip on the same individuals[45]. Genotyping accuracy based on 3,841 common positions was very high, with a mean value of 0.96 and a median value of 0.99. The imputed set of SNP was then annotated using Annovar[49] in order to group the SNPs per gene model of *P. trichocarpa* reference genome. For each SNP, we computed the overall genetic diversity statistic with the hierfstat R package[50] and this statistic was then averaged by gene model in order to get information on the extent of diversity. We further computed PCadapt score with the pcadapt R package[28] with 8 retained principal components. Here again, PCadapt scores were then summarized (averaged) by gene model in order to get information about their potential involvement in adaptation. Based on the principal component analysis, PCadapt is more powerful to perform genome scans for selection in next-generation sequencing data than approaches based on F_{ST} outliers detection[28]. We found a

bioRxiv preprint doi: https://doi.org/10.1101/523365; this version posted January 17, 2019. The copyright holder for this preprint (which was not certified by peer review) is the author/funder, who has granted bioRxiv a license to display the preprint in perpetuity. It is made available under aCC-BY 4.0 International license.

positive correlation between F_{ST} and PCadapt score (data not shown), but PCadapt shows differences between Core, random and peripheral gene sets (**Figure 4D**) when F_{ST} does not.

Transcription factors enrichment analysis

We have tested each of the gene sets (core, peripheral, Boruta, random) for enrichment in transcription factors, with data coming from the plant TFDB[51]. We selected in each set transcripts based on loci, regardless of the transcription factor families sharing different versions of the gene. Fisher's exact test was performed with the base R function fisher.test.

Data Availability

This RNAseq project is under submission to the international repository Gene Expression Omnibus (GEO) from NCBI. All steps of the experiment, from growth conditions to bioinformatic analyses are detailed in CATdb[52] according to the MINSEQE "minimum information about a high-throughput sequencing experiment". Raw sequences (fastq) are being deposited in the Sequence Read Archive (SRA) from NCBI. Information on the studied genotypes is available in GnpIS[53] at the following address:
https://urgi.versailles.inra.fr/gnpis-core/#form/crops=Forest%20tree&germplasmLists=POPULUS_NIGRA_RNASEQ_PANEL.

Figure Legends

Figure 1 WGCNA analysis of gene expression data. (A) Selection of the soft threshold (green dot) based on the correlation maximization with scale-free topology (left panel) producing low mean connectivity (right panel). (B) Gene expression hierarchical clustering dendrogram, based on the Spearman correlations (top panel), resulting in clusters identified by colors (first line of the bottom panel). Spearman correlations between gene expressions and traits are represented as color bands on the other lines of the bottom panel, from highly negative correlations (dark blue) to highly positive correlations (light yellow), according to the scale displayed in panel C. (C) Spearman correlation between eigengenes (the best theoretical representative of a gene expression module) of modules identified in the previous panel and traits, again on a dark blue (highly negative) to light yellow (highly positive) scale. (D) Focus on two modules from the previous graph, representing the correlations between gene expression correlation with mean sample diameter and centrality in the module. These two panels represent the strongest (left panel, black module, $R^2 = 0.66$) and the weakest (right panel, midnightblue module, $R^2 = 0.09$) correlations with the corresponding trait.

Figure 2 Predictions scores on test sets (R^2 on the y axis) for the 2 algorithms (LM Ridge, top panel; neural network, bottom panel) for each phenotypic trait (on the x axis). The color of each bar represents the gene set that has been used for the prediction. Intervals for the random set represent the first and third quartiles of the distribution of the 100 different realizations, while the height of the bar corresponds to the median.

bioRxiv preprint doi: https://doi.org/10.1101/523365; this version posted January 17, 2019. The copyright holder for this preprint (which was not certified by peer review) is the author/funder, who has granted bioRxiv a license to display the preprint in perpetuity. It is made available under aCC-BY 4.0 International license.

Figure 3 Difference of prediction scores (on the y-axis) between the core and peripheral gene sets (in blue) or between random sets (in green), for additive (LM Ridge in saturated colors) and interactive (neural network in faded colors) algorithms, for the different traits (on the x-axis). For the random pairs, error bars represent the first and third quartiles of the differences between pairs of randomized sets and the bar corresponds to the median.

Figure 4 (a) Heritability h^2, (b) gene expression (in counts per million), (c) differentiation Q_{ST}, (d) PCadapt score, (e) genetic variation coefficient CV_G and (f) overall gene diversity Ht violin plots for each of the core (in blue), random (in grey) and peripheral (in brown) gene sets. ns: p > 0.05, *: p <= 0.05, **: p <= 0.01, ***: p <= 0.001, ****: p <= 0.0001 by Wilcoxon rank-sum test.

Figure 5 An expanded view of the omnigenic model which handles the observed paradox between connectivity and interactivity. The dots correspond to genes colored according to their connectivity within the network, with core genes in blue and peripheral genes in brown. Stars correspond to transcription factors and arrows represent connections within the network. Hypothetical metabolic pathways are displayed in grey in order to show the upstream-downstream positions of peripheral and core genes, respectively.

References

1. Boyle, E. A., Li, Y. I. & Pritchard, J. K. An Expanded View of Complex Traits: From Polygenic to Omnigenic. *Cell* **169**, 1177–1186 (2017).
2. Maher, B. Personal genomes: The case of the missing heritability. *Nature* **456**, 18–21 (2008).
3. Josephs, E. B., Wright, S. I., Stinchcombe, J. R. & Schoen, D. J. The relationship between selection, network connectivity, and regulatory variation within a population of Capsella grandiora. *Genome Biol. Evol.* (2017). doi:10.1093/gbe/evx068
4. Josephs, E. B., Lee, Y. W., Stinchcombe, J. R. & Wright, S. I. Association mapping reveals the role of purifying selection in the maintenance of genomic variation in gene expression. *Proc. Natl. Acad. Sci. U. S. A.* **112**, 15390–15395 (2015).
5. Langfelder, P. & Horvath, S. WGCNA: an R package for weighted correlation network analysis. *BMC Bioinformatics* **9**, 559 (2008).
6. Williamson, S. H. *et al.* Simultaneous inference of selection and population growth from patterns of variation in the human genome. *Proc. Natl. Acad. Sci. U. S. A.* **102**, 7882–7887 (2005).
7. Sicard, A. *et al.* Divergent sorting of a balanced ancestral polymorphism underlies the establishment of gene-flow barriers in Capsella. *Nat. Commun.* **6**, 7960 (2015).
8. Mähler, N. *et al.* Gene co-expression network connectivity is an important determinant of selective constraint. *PLoS Genet.* **13**, e1006402 (2017).
9. Yu, H.-S. *et al.* Evidence of selection at melanin synthesis pathway loci during silkworm domestication. *Mol. Biol. Evol.* **28**, 1785–1799 (2011).
10. Lu, Y. & Rausher, M. D. Evolutionary rate variation in anthocyanin pathway genes. *Mol. Biol. Evol.* **20**, 1844–1853 (2003).
11. Rausher, M. D., Lu, Y. & Meyer, K. Variation in constraint versus positive selection as an explanation for evolutionary rate variation among anthocyanin genes. *J. Mol. Evol.* **67**, 137–

bioRxiv preprint doi: https://doi.org/10.1101/523365; this version posted January 17, 2019. The copyright holder for this preprint (which was not certified by peer review) is the author/funder, who has granted bioRxiv a license to display the preprint in perpetuity. It is made available under aCC-BY 4.0 International license.

144 (2008).
12. Rausher, M. D., Miller, R. E. & Tiffin, P. Patterns of evolutionary rate variation among genes of the anthocyanin biosynthetic pathway. *Mol. Biol. Evol.* **16**, 266–274 (1999).
13. Riley, R. M., Jin, W. & Gibson, G. Contrasting selection pressures on components of the Ras-mediated signal transduction pathway in Drosophila. *Mol. Ecol.* **12**, 1315–1323 (2003).
14. Han, M. *et al.* Evolutionary rate patterns of genes involved in the Drosophila Toll and Imd signaling pathway. *BMC Evol. Biol.* **13**, 245 (2013).
15. Song, X., Jin, P., Qin, S., Chen, L. & Ma, F. The evolution and origin of animal Toll-like receptor signaling pathway revealed by network-level molecular evolutionary analyses. *PLoS One* **7**, e51657 (2012).
16. Wu, X. *et al.* The evolutionary rate variation among genes of HOG-signaling pathway in yeast genomes. *Biol. Direct* **5**, 46 (2010).
17. Jovelin, R. & Phillips, P. C. Expression level drives the pattern of selective constraints along the insulin/Tor signal transduction pathway in Caenorhabditis. *Genome Biol. Evol.* **3**, 715–722 (2011).
18. Duret, L. & Mouchiroud, D. Determinants of substitution rates in mammalian genes: expression pattern affects selection intensity but not mutation rate. *Mol. Biol. Evol.* **17**, 68–74 (2000).
19. Pál, C., Papp, B. & Hurst, L. D. Highly expressed genes in yeast evolve slowly. *Genetics* **158**, 927–931 (2001).
20. Drummond, D. A., Bloom, J. D., Adami, C., Wilke, C. O. & Arnold, F. H. Why highly expressed proteins evolve slowly. *Proc. Natl. Acad. Sci. U. S. A.* **102**, 14338–14343 (2005).
21. Montanucci, L., Laayouni, H., Dall'Olio, G. M. & Bertranpetit, J. Molecular evolution and network-level analysis of the N-glycosylation metabolic pathway across primates. *Mol. Biol. Evol.* **28**, 813–823 (2011).
22. Bloom, J. D. & Adami, C. Evolutionary rate depends on number of protein-protein interactions independently of gene expression level: response. *BMC Evol Biol* **4**, 14 (2004).
23. Fraser, H. B. & Hirsh, A. E. Evolutionary rate depends on number of protein-protein interactions independently of gene expression level. *BMC Evol Biol* **4**, 13 (2004).
24. Gebreselassie, M. N. *et al.* Near-infrared spectroscopy enables the genetic analysis of chemical properties in a large set of wood samples from Populus nigra (L.) natural populations. *Ind. Crops Prod.* **107**, 159–171 (2017).
25. Muñoz, F. & Sanchez-Rodriguez, L. *breedR: Statistical Methods for Forest Genetic Resources Analysts*. (2018).
26. Kursa, M. B. & Rudnicki, W. R. Feature Selection with the Boruta Package. *J. Stat. Softw.* **36**, 1–13 (2010).
27. González-Recio, O., Rosa, G. J. M. & Gianola, D. Machine learning methods and predictive ability metrics for genome-wide prediction of complex traits. *Livest. Sci.* **166**, 217–231 (2014).
28. Luu, K., Bazin, E. & Blum, M. G. B. pcadapt: an R package to perform genome scans for selection based on principal component analysis. *Mol. Ecol. Resour.* **17**, 67–77 (2017).
29. de Los Campos, G., Hickey, J. M., Pong-Wong, R., Daetwyler, H. D. & Calus, M. P. L. Whole-genome regression and prediction methods applied to plant and animal breeding. *Genetics* **193**, 327–345 (2013).
30. Cordell, H. J. Epistasis: what it means, what it doesn't mean, and statistical methods to detect it in humans. *Hum. Mol. Genet.* **11**, 2463–2468 (2002).
31. Guet, J. *et al.* Genetic variation for leaf morphology, leaf structure and leaf carbon isotope discrimination in European populations of black poplar (Populus nigra L.). *Tree Physiol.* **35**, 850–863 (2015).
32. Dillen, S. Y., Marron, N., Sabatti, M., Ceulemans, R. & Bastien, C. Relationships among productivity determinants in two hybrid poplar families grown during three years at two

bioRxiv preprint doi: https://doi.org/10.1101/523365; this version posted January 17, 2019. The copyright holder for this preprint (which was not certified by peer review) is the author/funder, who has granted bioRxiv a license to display the preprint in perpetuity. It is made available under aCC-BY 4.0 International license.

contrasting sites. *Tree Physiol.* **29**, 975–987 (2009).
33. Langmead, B. & Salzberg, S. L. Fast gapped-read alignment with Bowtie 2. *Nat. Methods* **9**, 357–359 (2012).
34. Robinson, M. D. & Oshlack, A. A scaling normalization method for differential expression analysis of RNA-seq data. *Genome Biol.* **11**, R25 (2010).
35. Law, C. W., Chen, Y., Shi, W. & Smyth, G. K. voom: precision weights unlock linear model analysis tools for RNA-seq read counts. *Genome Biol.* **15**, R29 (2014).
36. Ritchie, M. D., Holzinger, E. R., Li, R., Pendergrass, S. A. & Kim, D. Methods of integrating data to uncover genotype–phenotype interactions. *Nat. Rev. Genet.* **16**, 85–97 (2015).
37. Suzuki, R. & Shimodaira, H. *pvclust: Hierarchical Clustering with P-Values via Multiscale Bootstrap Resampling*. (2015).
38. Rau, A. & Maugis-Rabusseau, C. Transformation and model choice for RNA-seq co-expression analysis. *Brief. Bioinform.* **19**, 425–436 (2018).
39. Kohavi, R. & John, G. H. Wrappers for feature subset selection. *Artif. Intell.* **97**, 273–324 (1997).
40. Nilsson, R., Peña, J. M., Björkegren, J. & Tegnér, J. Consistent Feature Selection for Pattern Recognition in Polynomial Time. *J. Mach. Learn. Res.* **8**, 589–612 (2007).
41. LeDell, E. *et al. h2o: R Interface for 'H2O'*. (2018).
42. van den Boogaart, K. G., Tolosana-Delgado, R. & Bren, M. *compositions: Compositional Data Analysis*. (2018).
43. Hornik, K., Stinchcombe, M. & White, H. Multilayer feedforward networks are universal approximators. *Neural Netw.* **2**, 359–366 (1989).
44. Cybenko, G. Approximation by superpositions of a sigmoidal function. *Math. Control Signals Systems* **2**, 303–314 (1989).
45. Faivre-Rampant, P. *et al.* New resources for genetic studies in Populus nigra: genome-wide SNP discovery and development of a 12k Infinium array. *Mol. Ecol. Resour.* **16**, 1023–1036 (2016).
46. Speed, D., Hemani, G., Johnson, M. R. & Balding, D. J. Improved heritability estimation from genome-wide SNPs. *Am. J. Hum. Genet.* **91**, 1011–1021 (2012).
47. Rogier, O. *et al.* Accuracy of RNAseq based SNP discovery and genotyping in Populus nigra. *BMC Genomics* **19**, 909 (2018).
48. Sargolzaei, M., Chesnais, J. P. & Schenkel, F. S. A new approach for efficient genotype imputation using information from relatives. *BMC Genomics* **15**, 478 (2014).
49. Wang, K., Li, M. & Hakonarson, H. ANNOVAR: functional annotation of genetic variants from high-throughput sequencing data. *Nucleic Acids Res.* **38**, e164 (2010).
50. Goudet, J. & Jombart, T. hierfstat: estimation and tests of hierarchical F-statistics. *R package version 0. 04-22* (2015).
51. Jin, J. *et al.* PlantTFDB 4.0: toward a central hub for transcription factors and regulatory interactions in plants. *Nucleic Acids Res.* **45**, D1040–D1045 (2017).
52. Gagnot, S. *et al.* CATdb: a public access to Arabidopsis transcriptome data from the URGV-CATMA platform. *Nucleic Acids Res.* **36**, D986–90 (2008).
53. Steinbach, D. *et al.* GnpIS: an information system to integrate genetic and genomic data from plants and fungi. *Database* **2013**, bat058 (2013).

Acknowledgements

The authors gratefully acknowledge the staff of the INRA GBFOR experimental unit for the establishment and management of the poplar experimental design in Orléans, the collection of wood samples in each site, and their contribution to phenotypic measurements on poplars in

bioRxiv preprint doi: https://doi.org/10.1101/523365; this version posted January 17, 2019. The copyright holder for this preprint (which was not certified by peer review) is the author/funder, who has granted bioRxiv a license to display the preprint in perpetuity. It is made available under aCC-BY 4.0 International license.

Orléans; Alasia Franco Vivai staff for management of the poplar experimental plantation in Savigliano, and M. Sabatti and F. Fabbrini for their contribution to phenotypic measurements on poplars in Savigliano. We acknowledge the staff of BioForA for their contribution to RNA collection in the field. We would also like to thank M. Nordborg for useful discussions on this work and J. Salse for useful comments on the manuscript. Establishment and management of the experimental sites were carried out with financial support from the NOVELTREE project (EU-FP7-211868). RNA collection, extraction, and sequencing were supported by the SYBIOPOP project (ANR-13-JSV6-0001) funded by the French National Research Agency (ANR). The platform POPS benefits from the support of the LabEx Saclay Plant Sciences-SPS (ANR-10-LABX-0040-SPS).

Author contributions

AC, LS, and VS designed the experiment, discussed the results and wrote this manuscript. AC ran the in silico experiment. MCL, VB, CPL, LT, MLMM, and VS contributed the RNAseq data production and analysis. VJ, OR and VS contributed to the SNP data production and analysis. MLMM and JCL contributed to the discussion on the methodology employed. All the authors read and approved this manuscript.

Competing financial interests

No competing financial interest has been declared by the authors.

Materials & Correspondence

To whom correspondence should be addressed: vincent.segura@inra.fr

bioRxiv preprint doi: https://doi.org/10.1101/523365; this version posted January 17, 2019. The copyright holder for this preprint (which was not certified by peer review) is the author/funder, who has granted bioRxiv a license to display the preprint in perpetuity. It is made available under aCC-BY 4.0 International license.

Figures

Figure 1

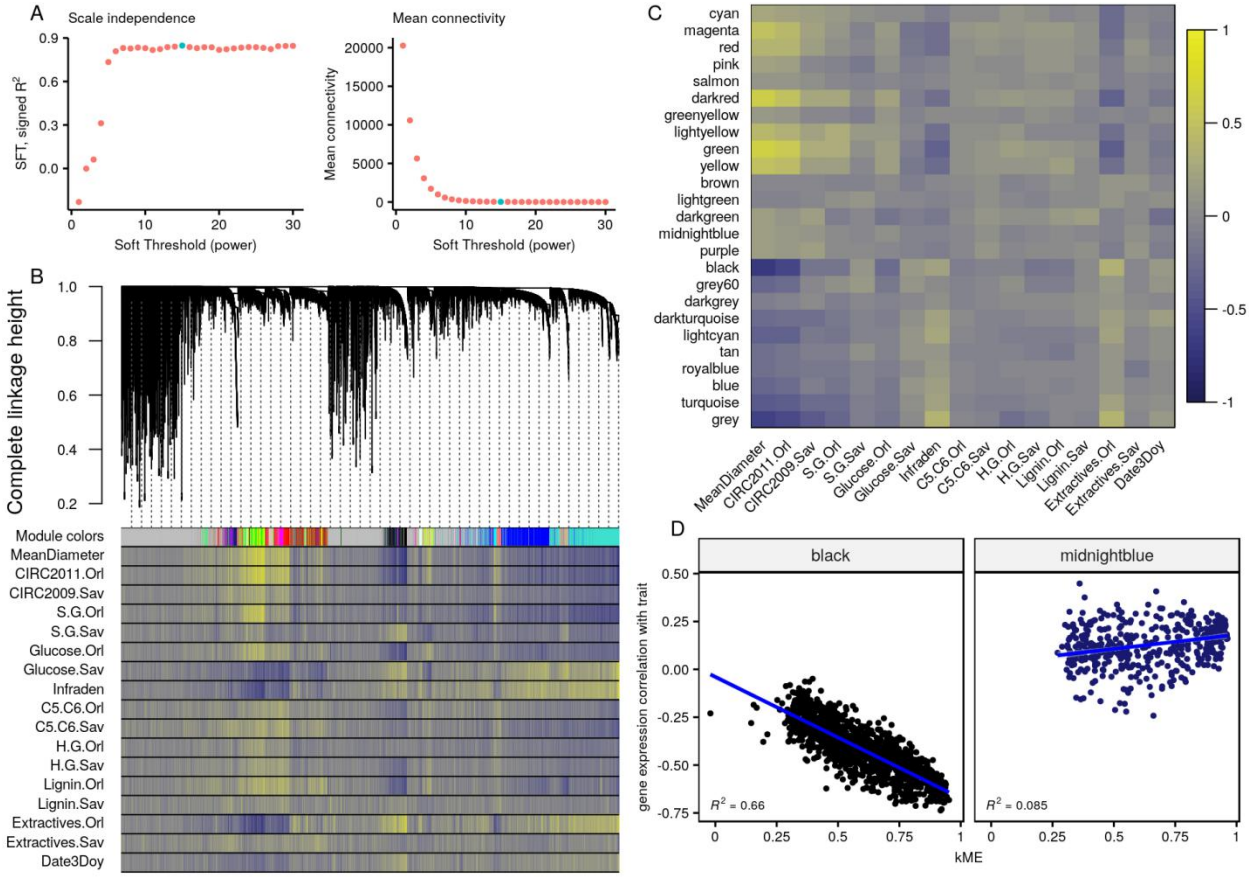

bioRxiv preprint doi: https://doi.org/10.1101/523365; this version posted January 17, 2019. The copyright holder for this preprint (which was not certified by peer review) is the author/funder, who has granted bioRxiv a license to display the preprint in perpetuity. It is made available under aCC-BY 4.0 International license.

Figure 2

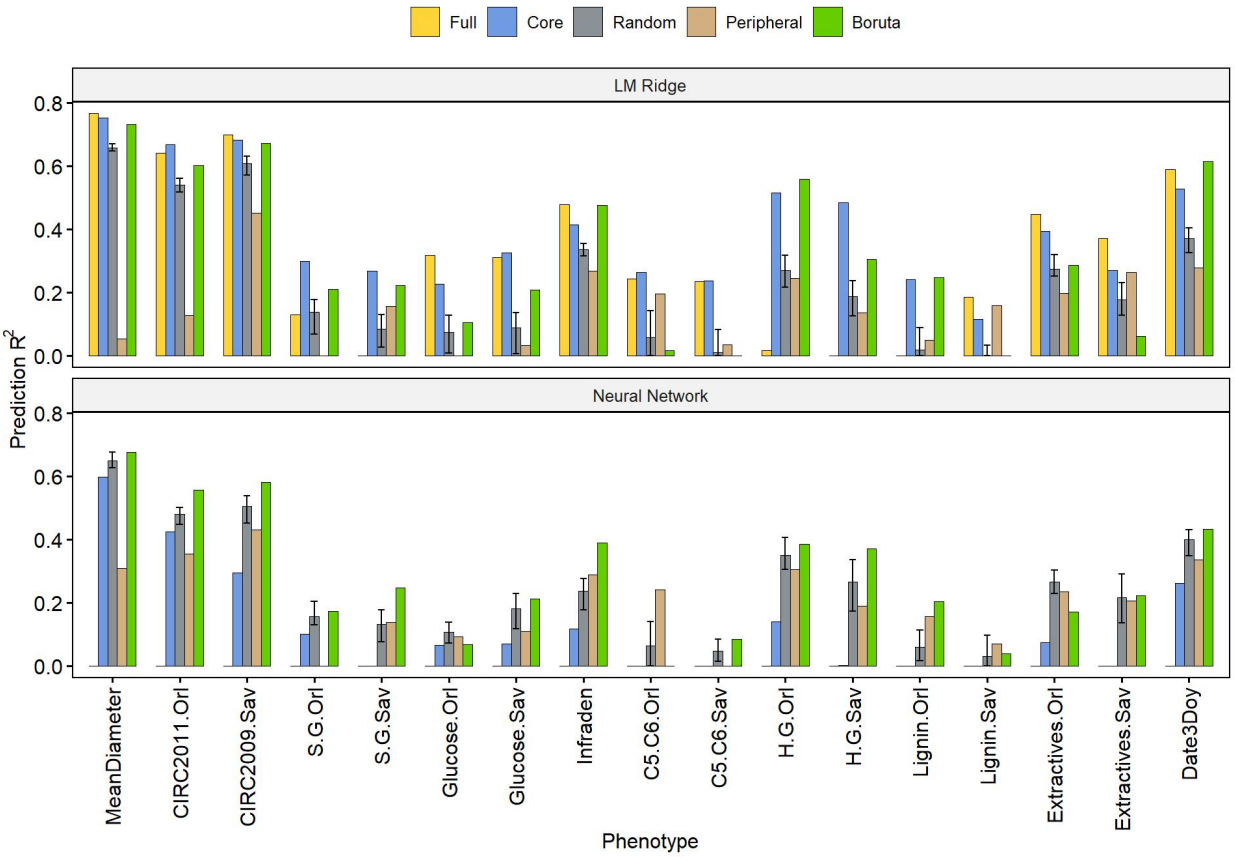

bioRxiv preprint doi: https://doi.org/10.1101/523365; this version posted January 17, 2019. The copyright holder for this preprint (which was not certified by peer review) is the author/funder, who has granted bioRxiv a license to display the preprint in perpetuity. It is made available under aCC-BY 4.0 International license.

Figure 3

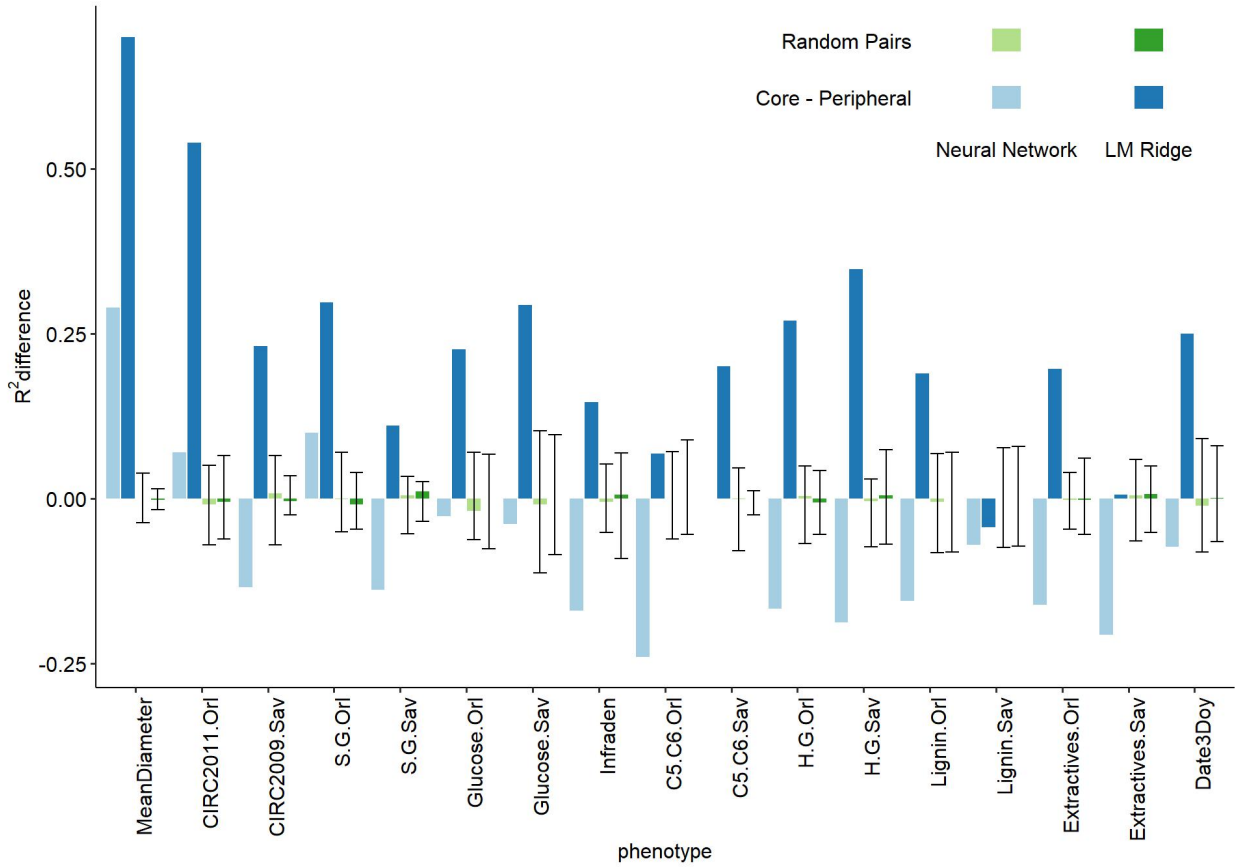

bioRxiv preprint doi: https://doi.org/10.1101/523365; this version posted January 17, 2019. The copyright holder for this preprint (which was not certified by peer review) is the author/funder, who has granted bioRxiv a license to display the preprint in perpetuity. It is made available under aCC-BY 4.0 International license.

Figure 4

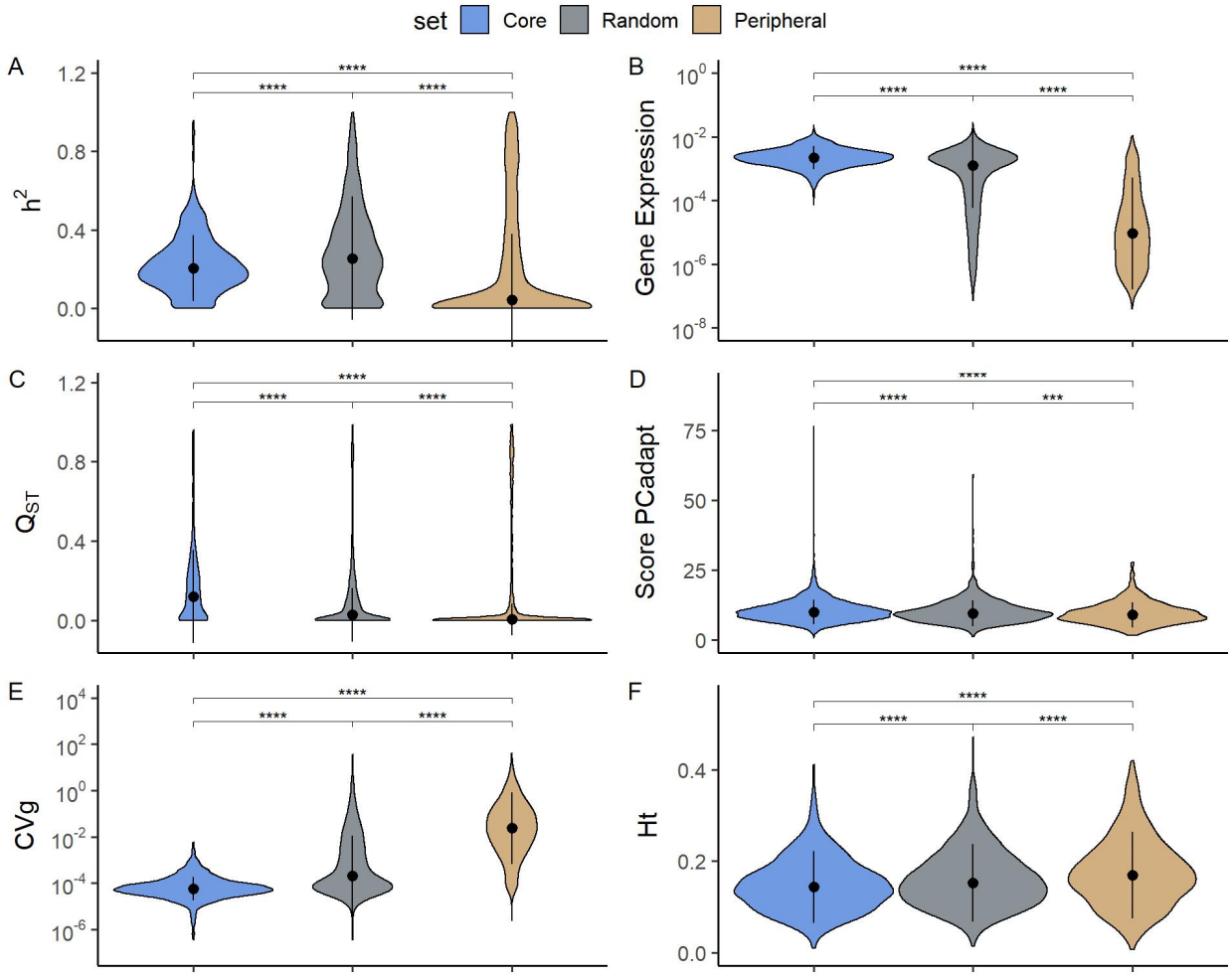

bioRxiv preprint doi: https://doi.org/10.1101/523365; this version posted January 17, 2019. The copyright holder for this preprint (which was not certified by peer review) is the author/funder, who has granted bioRxiv a license to display the preprint in perpetuity. It is made available under aCC-BY 4.0 International license.

Figure 5